

ASXL1 mutations in AML are associated with a distinct epigenetic state that results in vulnerabilities to epigenetic-targeted agents

Christopher Peter Mill, PhD, BA[1], Warren C. Fiskus, BSc, PhD[1], Christine Birdwell, PhD[1], John A. Davis[1], Kaberi Das, PhD[1], Hanxi Hou[1], Surbhi Sharma, PhD[1], Koji Sasaki, MD[1], Sanam Loghavi, MD[2], Tapan M. Kadia, MD[1], Naval Daver, MD[1], Courtney D. DiNardo, MD, MSc[1], Lu Wang, PhD[3] and Kapil N. Bhalla, MD[1]

[1]Department of Leukemia, University of Texas MD Anderson Cancer Center, Houston, TX; [2]Department of Hematopathology, University of Texas MD Anderson Cancer Center, Houston, TX; [3]Department of Biochemistry and Molecular Genetics, Northwestern University, Chicago, IL

THE UNIVERSITY OF TEXAS MD Anderson Cancer Center

Introduction

Hematopoietic cells frequently acquire mutations in epigenetic regulators as they transform from normal to a pre-leukemic (myeloproliferative neoplasms – MPN, myelodysplastic syndromes – MDS) state and accumulate additional mutations as they progress to acute myeloid leukemia (AML). These genetic mutations alter the epigenetic landscape within a cell, which may result in silencing of tumor suppressors and aberrant expression of proliferative, pro-survival, and transcription-associated genes leading to a malignant phenotype. Several genes (e.g. DNMT3A, TET2, ASXL1, JAK2, SF3B1, SRSF2) when mutated offer the hematopoietic progenitor cell a competitive advantage; and this class of genetic mutations are often referred to as CHIP (clonal hematopoiesis of indeterminate potential) mutations, which result in a shift to the pre-leukemic state. Specifically, mutations in ASXL1 confer a poor prognosis in patients with myeloid malignancies. In addition, knock-in (KI) mouse models have shown that deregulated transcription caused by mutant ASXL1 leads to impaired erythroid differentiation. ASXL1 is often mutated in MPN (5%−11%), MDS (14%−23%), chronic myelomonocytic leukemia (CMML, 40%−49%), and AML (5%−17%). ASXL1 mutations commonly occur within the last exon (12) resulting in a frameshift or nonsense mutation causing a truncation of the ASXL1 protein.

While it has no enzymatic activity, ASXL1 acts as a scaffold protein for multiple epigenetic complexes. One family of chromatin regulators that interact with ASXL1, is the Polycomb group (PcG), an essential regulator of differentiation. These chromatin regulator complexes modify the chromatin landscape by altering the methylation or ubiquitylation of specific histone lysine residues (e.g. H3K27me3 by PRC (Polycomb Repressive Complex) 2 and H2AK119Ub by PRC1). Noth H3K27me3 and H2AK119Ub are suppressive histone marks and result in silencing of gene transcription. On the other hand, Polycomb Repressive-Deubiquitinase (PR-DUB) complex, trithorax group (TrxG), and KDM/HAT (UTX/P300) offer a counterbalance either by removing suppressive or adding permissive histone marks (e.g. H3K4me1 and H3K27Ac). ASXL1 functions as a scaffold in both the PRC2 (reducing transcription) and the PR-DUB complex (enhancing transcription), potentially playing a role in enhancing or suppressing transcription depending on the context. The loss of ASXL1 in mouse models, AML cell lines, and CD34+ cord blood or knock-in of truncating ASXL1 mutations has been correlated with a reduction in global H3K27me3 levels. In addition, knock-in (KI) of an ASXL1 nonsense mutation results in an increase in global H3K27Ac levels. While not definitive, taken together these data suggest that mutations in ASXL1 result in a loss-of-function (LOF) phenotype in the context of PRC2. Conversely, ASXL1 mutations have been associated with a gain-of-function (GOF) phenotype in the context of PR-DUB. KI of the truncated ASXL1 gene into normal progenitors (cord blood) leads to global alterations in the H2AK119Ub mark as well as increases in myeloid and stem cell gene expressions. A known target of PRC1, p16^{Ink4a} (CDKN2A), has also been shown to be de-repressed by the introduction of mutant (mt) ASXL1. Additionally, the PR-DUB complex can recruit TrxG (MLL3/4) and UTX to regulate H3K4me1 and H3K27me3 histone marks, respectively. In addition to functioning as a scaffold for PcG, truncated ASXL1, but not wild-type (wt) ASXL1 binds to (co-IPs) Brd4 protein. Consistent with this, ASXL1 transgenic mice (non-sense mutation) have an enhanced sensitivity to BET inhibitor treatment. Taken together, ASXL1 mutations and their altered function, modify chromatin state and dysregulate RNAPII pause release resulting in an upregulated transcriptome.

To determine the direct and specific effects of the presence of an ASXL1 mutations on the biology and therapeutic susceptibility of AML cells, we knocked-in the mutant ASXL1 Y591* in AML cells. Our findings demonstrate that knock-in of mutant ASXL1 resulted in increased expression of myeloid transcription factors (Myc, Myb, PU.1 and EVI1). Importantly, the introduction of mtASXL1 upregulated MYC targets and associated gene-set (via gene set enrichment analysis – GSEA), as determined from data derived from mass spectrometry. In addition, the mutant ASXL1 introduction altered the epigenetic landscape, e.g., down regulating H2AK119Ub and upregulating BAP1 and H3K27Ac at several loci, including RXRA gene and at many genes within the Wnt/β-catenin stem cell pathway (WNT7B, WNT5B, FZD1, APC, BCL9L, DVL1 and TCF7L2). Following the knock-in of the mutant ASXL1, the ranked ordering of super-enhancers (ROSE) analysis of the signal density and intensity demonstrated that the ranking of the RXRA super-enhancer was increased, and a super-enhancer was gained for TCF7L2. Notably, KI of mtASXL1 resulted in resistance to standard AML therapies (e.g., Etoposide, Cytarabine and Daunorubicin), supporting the need to identify alternative and more targeted therapies. To address this need and based on the dysregulated gene expressions induced in AML cells by mtASXL1, we determined the effects of BET, HAT, dual BET/HAT, and mediator kinase inhibitors on AML cells in AML cells with mtASXL1. Our findings confirmed that the KI of mutant ASXL1 in AML cells increased their sensitivity to BET inhibitors, and identified additional vulnerabilities to HAT inhibitors, the mediator kinase inhibitor (SEL120-34A/RVU120), as well as to a dual BET/HAT inhibitor (NEO2734/EP31670). Treatment with NEO2734 reduced the mRNA and protein expressions of a large cohort of genes that were upregulated by KI of mtASXL1, especially those within the MYC pathway. Inhibition of the mediator kinases (CDK8/19) with SEL120-34A altered the expressions of several chromatin modifiers (e.g., EP300/CREBBP and ARID1B/2) as well as of RARA and RARG, which were genes upregulated by the KI of mtASXL1. Based on this, we also determined that treatment with NEO2734, pelabresib, or SEL120-34A induced lethality in cell lines and patient-derived (PD) AML samples harboring mtASXL1. Collectively, these findings highlight that rational NEO2734-based combinations could potentially exert significant anti-AML efficacy against AML cells with mutant ASXL1.

Results

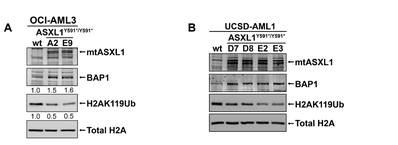


Figure 1. Knock-in (KI) of mutant (mt) ASXL1 Stabilizes BAP1 Expression Leading to Reduced H2AK119Ub. A. and **B.** Immunoblot analysis of parental and isogenic mutant ASXL1 KI OCI-AML3 (clones A2 & E9) and UCSD-AML1 (clones D7, D8, E2, E3) cells in exponential phase. Total H2A protein expression served as the loading control.

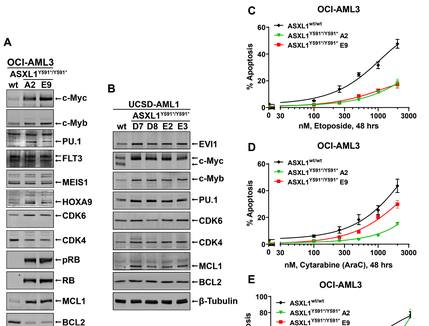


Figure 2. KI of mtASXL1 Increased Expression of c-Myc, c-Myb, and PU.1 and Led to Resistance to Standard AML Therapies. A. and **B.** Immunoblot analysis of parental and isogenic mutant ASXL1 KI OCI-AML3 (clones A2 & E9) and UCSD-AML1 (clones D7, D8, E2, E3) cells in exponential phase. β-tubulin expression served as the loading control. **C-E.** OCI-AML3 parental and ASXL1 KI cells were treated with the indicated concentrations of etoposide, cytarabine, or daunorubicin for 48 hours. At the end of treatment, cells were stained with Annexin V and ToPro-3 iodide and the percentage of apoptotic cells were determined by flow cytometry. Curves represent means of three independent experiments. Error bars represent S.E.M.

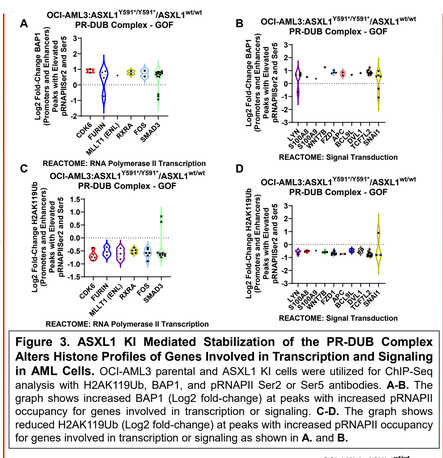


Figure 3. ASXL1 KI Mediated Stabilization of the PR-DUB Complex Alters Histone Profiles of Genes Involved in Transcription and Signaling in AML Cells. OCI-AML3 parental and ASXL1 KI cells were utilized for ChIP-Seq analysis with H2AK119Ub, BAP1, and pRNAPII Ser2 or Ser5 antibodies. **A-B.** The graph shows increased BAP1 (Log2 fold-change) at peaks with increased pRNAPII occupancy for genes involved in transcription or signaling. **C-D.** The graph shows reduced H2AK119Ub (Log2 fold-change) at peaks with increased pRNAPII occupancy for genes involved in transcription or signaling as shown in **A.** and **B.**

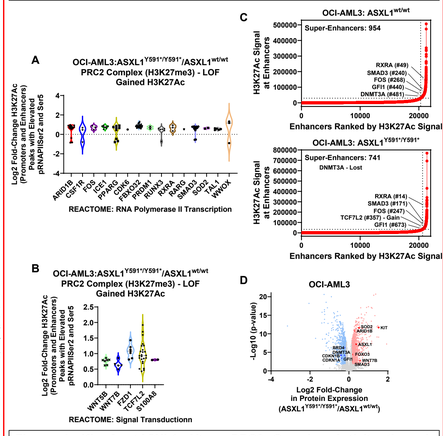


Figure 4. KI of mtASXL1 Alters PRC2 Complex Activity through Increased H3K27Ac Occupancy at Loci and Protein Expression of Genes Involved in Transcription and Signaling in AML Cells. A. and **B.** OCI-AML3 parental and ASXL1 KI cells were utilized for ChIP-Seq analysis with H3K27Ac and pRNAPII Ser2 or Ser5 antibodies. The graphs show increased H3K27Ac (Log2 fold-change) at peaks with increased pRNAPII occupancy for genes involved in transcription or signaling. **C.** Ranked ordering of super enhancers (ROSE) analysis of H3K27Ac ChIP-Seq peak density in OCIAML3 ASXL1 KI or parental cells. **D.** Volcano plot shows Log2 fold-change versus –Log10 p-value for transcription and signaling-related genes.

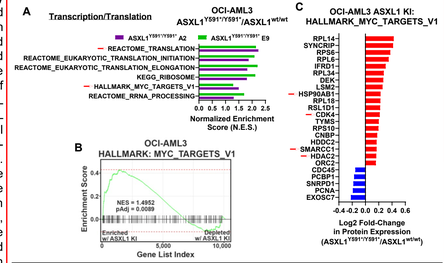


Figure 5. KI of mtASXL1 Altered Histone Profiles Led to Positive Enrichment of Transcription (MYC) and Translation Gene Sets. A. Gene set enrichment analysis (GSEA) of mass spectrometry (M/S) determined differences in OCI-AML3 ASXL1 KI over parental cells. Graph shows normalized enrichment scores for each gene set at F.D.R. q-value < 0.1. **B.** GSEA enrichment plot of M/S determined protein expression changes compared to HALLMARK MYC_TARGETS_V1. **C.** Log2 fold-change of selected proteins in OCI-AML3 ASXL1 KI over parental within HALLMARK MYC_TARGETS_V1 gene set.

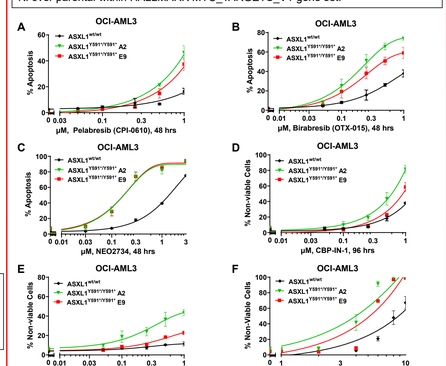


Figure 6. Differential Response of mtASXL1 KI AML cells to Chemotherapeutic and Selected Epigenetic Targeted Agents. A-C. OCI-AML3 parental and ASXL1 KI cells were treated with the indicated concentrations of pelabresib, birabresib or NEO2734/EP31670 for 48 hours. At the end of treatment, cells were stained with Annexin V and ToPro-3 iodide and the percentage of apoptotic cells were determined by flow cytometry. Curves represent means of three independent experiments. Error bars represent S.E.M. **D-F.** OCI-AML3 parental and ASXL1 KI cells were treated with the indicated concentrations of CBP-IN-1, GNE-781, and SEL120-34A/RVU120 for 96 hours. At the end of treatment, cells were stained with ToPro-3 iodide and the percentage of non-viable cells were determined by flow cytometry. Curves represent means of three independent experiments. Error bars represent S.E.M.

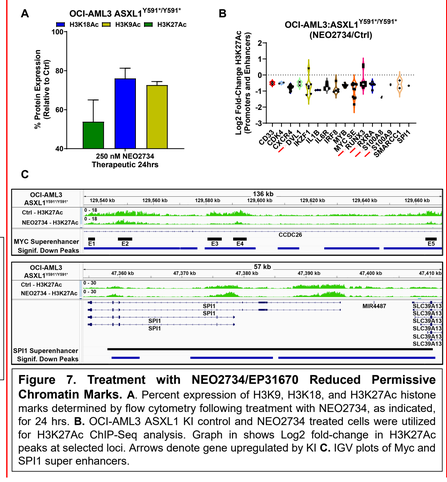


Figure 7. Treatment with NEO2734/EP31670 Reduced Permissive Chromatin Marks. A. Percent expression of H3K9, H3K18, and H3K27Ac histone marks determined by flow cytometry following treatment with NEO2734, as indicated, for 24 hrs. **B.** OCI-AML3 ASXL1 KI control and NEO2734 treated cells were utilized for H3K27Ac ChIP-Seq analysis. Graph in shows Log2 fold-change in H3K27Ac peaks at selected loci. Arrows denote gene upregulated by KI **C.** IGV plots of Myc and SPI1 super enhancers.

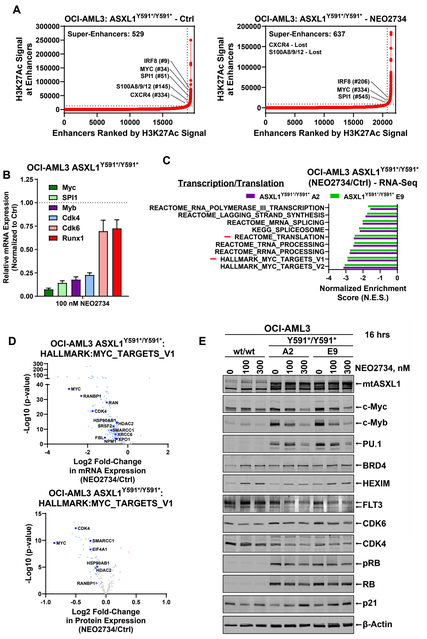


Figure 8. Treatment with NEO2734/EP31670 Reduced Permissive Chromatin Marks Leading to Negative Enrichment of Transcription (MYC) and Translation. A. ROSE analysis of H3K27Ac ChIP-Seq in OCIAML3 ASXL1 KI control or NEO2734 treated cells. **B.** Relative mRNA expression of leukemia relevant genes in OCI-AML3 ASXL1 KI cells following treatment with 100 nM of NEO2734 for 16 hrs. **C.** Gene set enrichment analysis (GSEA) of RNA-Seq determined differences in NEO2734-treated over control OCI-AML3 ASXL1 KI cells. Graph shows normalized enrichment scores for each gene set at F.D.R. q-value < 0.1. Volcano plots in **D.** shows Log2 fold-change versus –Log10 p-value for genes (mRNA & Protein) within the MYC_TARGETS_V1 data set. **E.** Immunoblot analysis of OCI-AML3 parental and ASXL1 KI cells treated with the indicated concentrations of NEO2734 for 16 hrs.

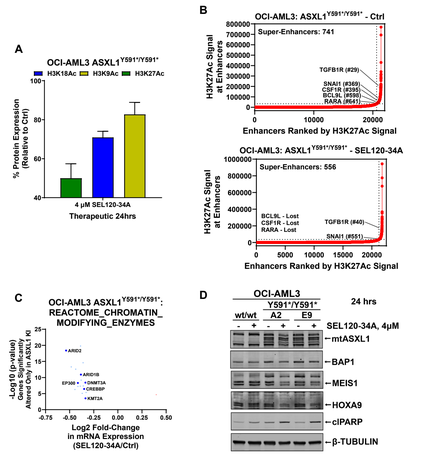


Figure 9. Treatment with SEL120-34A/RVU120 Reduced Permissive Chromatin Marks Leading to Reduction in Chromatin Modifying Enzyme mRNA Expression and Decreased BAP1, MEIS1, and HOXA9 Proteins in mtASXL1 KI OCI-AML3 Cells. A. Percent expression of H3K9, H3K18, and H3K27Ac histone marks determined by flow cytometry following treatment with SEL120-34A, as indicated, for 24 hrs. **B.** ROSE analysis of H3K27Ac ChIP-Seq in OCIAML3 ASXL1 KI control or NEO2734 treated cells. **C.** Volcano plot of the Log2 fold-change of selected genes in SEL120-34A treated over control OCI-AML3 ASXL1 KI cells within the REACTOME_CHROMATIN_MODIFYING_ENZYMES gene set. **D.** Immunoblot analysis of OCI-AML3 parental and ASXL1 KI treated with the indicated concentrations of SEL120-34A for 24 hrs.

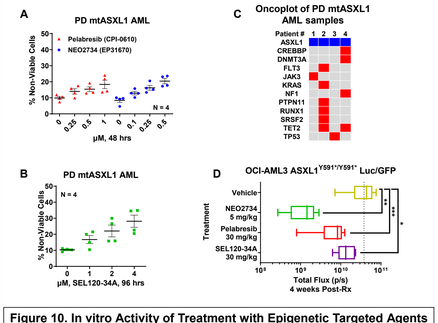


Figure 10. In vitro Activity of Treatment with Epigenetic Targeted Agents Against PD mtASXL1-Expressing AML Samples. A. and **B.** Primary patient-derived (PD) mtASXL1 AML cells were treated with the indicated concentrations of pelabresib, NEO2734, and SEL120-34A for 48 or 96 hours as indicated. Following this the percentage of ToPro-3 iodide positive, non-viable cells were determined by flow cytometry. **C.** Oncoplot of mutations identified by Next-Generation Sequencing (NGS) in the patient-derived AML samples. **D.** Total bioluminescent flux (P/S) in NSG mice engrafted with (1.2 million) OCI-AML3 mtASXL1 KI cells and treated for four weeks as indicated. * p < 0.05; ** p < 0.005; *** p < 0.001

Conclusions

1. We created two isogenic knock-in (KI) cellular models of mtASXL1 Y591* in the AML cell lines OCI-AML3 and UCSD-AML1. These cells exhibit elevated expressions of the truncated ASXL1 and BAP1, associated with reduced H2AK119Ub histone mark.
2. The KI of mtASXL1 stabilized ASXL1/BAP1 in OCI-AML3 and UCSD-AML1 cells, as well as increased the expression of c-Myc protein. This was associated with upregulation of the MYC pathway proteins.
3. mtASXL1 KI in OCI-AML3 cells caused a reduced H2AK119Ub & elevated H3K27Ac occupancy on the chromatin of Wnt/β-catenin stem cell pathway genes.
4. Compared to the control OCI-AML3 cells, OCI-AML3 with mtASXL1 KI exhibited reduced sensitivity to standard AML drugs but demonstrated increased sensitivity to epigenetically targeted agents.
5. Treatment with NEO2734/EP31670 reduced the permissive chromatin marks associated with downregulation of the MYC pathway.
6. Treatment with SEL120-34A/RVU120 also reduced active chromatin marks in the mtASXL1 expressing AML cells. This was associated with reduced expression of BAP1, MEIS1 and HOXA9 proteins.
7. Treatment with NEO2734, pelabresib, and SEL120-34A induced in vitro lethality in patient derived mtASXL1-expressing AML samples. In addition, treatment with NEO2734, pelabresib, or SEL120-34A, significantly reduced AML burden in NSG mice engrafted with mtASXL1-expresssing OCI-AML3 cells.
8. Utilizing the isogenic models of AML cells expressing mtASXL1, collectively these findings support the rationale to evaluate dual HAT-BET inhibitor-based combination therapies against AML cells.